

Thin-foil expansion into a vacuum

P. Mora*

Centre de Physique Théorique (UMR 7644 du CNRS), Ecole Polytechnique, Palaiseau 91128, France

(Received 29 December 2004; published 15 November 2005)

The collisionless expansion into a vacuum of a thin foil heated by an ultrashort laser pulse and adiabatically cooling down is studied with a particular emphasis on the structure of the accelerating field and on the resultant ion energy spectrum. For late times, a double layer structure at the ion front becomes the dominant feature. The dependence of the maximum ion velocity on the thin foil width is established. The effect of a two-temperature electron distribution function is discussed.

DOI: 10.1103/PhysRevE.72.056401

PACS number(s): 52.38.Kd, 41.75.Jv, 52.40.Kh, 52.65.-y

There has been a large number of recent experiments showing ion acceleration in the interaction of ultrashort laser pulses with thin foils [1,2]. Three mechanisms are invoked to explain the ion acceleration [3], where the ions are accelerated by the charge separation created at the front side of the target, inside the target by a shock propagating across the plasma [4], or at the back of the target [5]. In the last case, the detailed mechanism is the following: fast electrons are first created at the target front side by the laser-plasma interaction. A crude estimate of the heated electron temperature is simply given by the energy of the electrons oscillating in the transverse field of the incident light wave [6], $k_B T_e = (\gamma - 1)m_e c^2$, where $\gamma = (1 + I\lambda^2 / 1.37 \times 10^{18})^{1/2}$, I is the intensity in Wcm^{-2} and λ is the wavelength in μm . The electrons then propagate through the target and build a charge separation field at the rear side. The corresponding electric field ionizes atoms and accelerates ions [7]. The ion expansion is commonly described by the model of free isothermal expansion into a vacuum of a plasma occupying initially a half space [8–10]. This model predicts an ion velocity spectrum with a high velocity cutoff, which is given by [10]

$$v_{max} \approx 2c_s \ln(\tau + \sqrt{\tau^2 + 1}), \quad (1)$$

where $c_s = (Zk_B T_e / m_i)^{1/2}$ is the ion-acoustic velocity, $\tau = \omega_{pi} t / \sqrt{2e_N}$, $\omega_{pi} = (n_{e0} Z e^2 / m_i \epsilon_0)^{1/2}$ is the ion plasma frequency, n_{e0} is the electron density in the unperturbed plasma, Z is the ion charge number, and $e_N = 2.71828\dots$. The maximum velocity in (1) diverges logarithmically with time, while the total energy in the fast ions diverges linearly, so that to be able to apply the model to the interpretation of experiments, one has to determine the relevant time t at which the acceleration is stopped. A natural choice for t is the laser pulse duration t_l [2], but one might argue that, in the experiment, the acceleration does not stop suddenly, and that it goes on even for $t > t_l$. On the other hand, the isothermal model assumes a constant electron temperature, which can be a reasonable assumption during the laser pulse, but is certainly violated for late times, as the electrons progressively give their energy to the ions [9] and cool down in the expansion. Remarkable exact self-similar solutions were

given in the quasineutral limit for the adiabatic plasma expansion of plasma bunches into vacuum [11]. However, these solutions require specific initial conditions, correlating the spatial and the velocity space (for instance, for Maxwellian distribution functions for the electrons and the single species ions, the density has to be Gaussian in space). Furthermore, they do not describe the charge separation effect and the structure of the ion front, which is crucial in the determination of the maximum velocity of accelerated ions.

In this paper, we propose an alternative model which treats the collisionless expansion into a vacuum of a thin foil of initial width L . The model fully takes into account the electron cooling due to the energy transfer to the ions and the charge separation effects. The most salient results of the present work are the prediction of a double layer structure of the ion front, significantly more pronounced than in the isothermal case, and the prediction of the maximum ion velocity as a function of the foil thickness.

At time $t=0$ the ions are cold and initially at rest with density $n_i = n_{i0} = n_{e0}/Z$ for $|x| < L/2$ and $n_i = 0$ for $|x| > L/2$ with sharp boundaries (in contrast with the initial conditions of the self-similar quasineutral solutions [11]). The expansion being symmetrical with respect to $x=0$, we only simulate the half space $x > 0$. The equations of the model are the Boltzmann equation for the electron density n_e , the Poisson equation for the electric potential Φ , and the equations of continuity and motion for the ion density n_i and the ion velocity v_i , and do not differ in this respect from the equations of the isothermal model [10]. However, the boundary condition is now different on the left part of the simulation box, since one has $E(x=0) = 0$ and $v_i(x=0) = 0$ for any time t . Furthermore, the electron temperature is now a function of time determined by the energy conservation equation,

$$dU_e/dt = -dU_{ions}/dt - dU_{field}/dt, \quad (2)$$

where U_{ions} is the kinetic energy of the ions, U_{field} is the electrostatic energy of the electric field, and $U_e = g(\theta)N_e k_B T_e$ is the thermal energy of the electrons (all these quantities are defined per unit surface). Here $N_e = n_{e0}L$ is the total number of electrons, and $g(\theta)$ is a function of $\theta = k_B T_e / m_e c^2$ with $g = 1/2$ in the classical limit ($\theta = 0$) and $g = 1$ in the ultrarelativistic limit ($\theta = \infty$). Alternatively, the thermal energy of the electrons can be calculated directly by

*Electronic address: mora@cphpt.polytechnique.fr

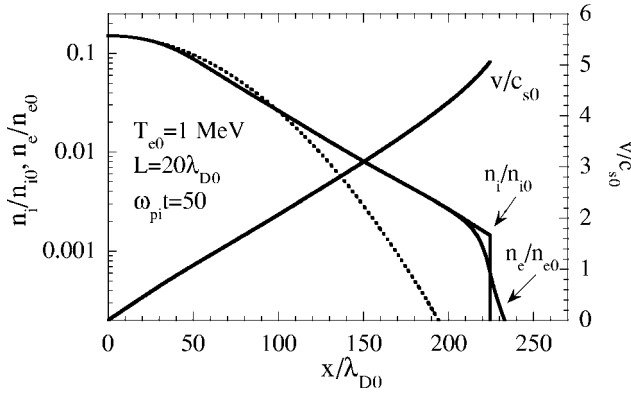


FIG. 1. Ion and electron densities and ion velocity as functions of x for $L=20\lambda_{D0}$ and $T_{e0}=1$ MeV, at time $\omega_{pi}t=50$ (i.e., $t=5t_L$). Also shown in dotted line is the best-fitted Gaussian density. Typical physical parameters for the hot electrons driving the expansion are $n_{e0}=10^{19}$ cm $^{-3}$, corresponding to $\omega_{pi}^{-1}=240$ fs (for protons) and $\lambda_{D0}=2.35$ μ m, in which case the above parameters correspond to $L=47$ μ m and $t=12$ ps.

the work done by the electric field on the electron fluid,

$$\begin{aligned} dU_e/dt &= -e \int_{-\infty}^{\infty} En_e v_e dx = -k_B T_e \int_{-\infty}^{\infty} n_e \partial v_e / \partial x dx \\ &= e \int_{-\infty}^{\infty} \Phi \partial n_e / \partial x dx. \end{aligned} \quad (3)$$

We have solved the system of equations with the Lagrangian code described in Ref. [10], to which the numerical resolution of Eqs. (2)–(3) has been added. Our model differs from the model of Ref. [12] in which v_e is replaced by v_i in Eq. (3). This replacement leads to significant differences for the thinner foils, when U_{field} is not negligible, and for two-temperature electron distribution functions. On the other hand, we have verified that our results agree with the published results of a particle-in-cell code [13] within 1%.

If the electron temperature was maintained constant by an external source of energy, it would take a time $t_L=L/2c_{s0}$, where c_{s0} is the initial ion-acoustic velocity, for the rarefaction wave to reach the center of the foil, and thus t_L is the relevant characteristic expansion time of the foil. Actually, for $t \ll t_L$, the expansion is not significantly different from the isothermal semi-infinite case. For $0 < t \lesssim t_L$, the cooling progressively occurs as evidenced in Ref. [13]. For $t \gg t_L$, the electron cooling is fully effective and the velocity becomes progressively frozen, with $v(x,t) \approx x/t$, as can be seen in Fig. 1, which shows at time $\omega_{pi}t=50$ (i.e., $t=5t_L$), the ion velocity and the ion and electron densities as functions of space, for $L=20\lambda_{D0}$ and $T_{e0}=1$ MeV, where λ_{D0} is the Debye length in the unperturbed plasma, $\lambda_{D0}=(\epsilon_0 k_B T_{e0}/n_{e0} e^2)^{1/2}$, and T_{e0} is the initial electron temperature. At that time, the electron temperature is only 4% of its initial value. Also shown in Fig. 1 in dotted line is the best-fitted Gaussian density which corresponds to the self-similar solutions of Ref. [11]. For $t \gg t_L$, the density profile becomes self-similar, with $n(x,t) = f(x/t)/t$, and the characteristic length $l_e(x,t) = |\partial \ln n_e / \partial x|^{-1}$ becomes a linear function of time, when con-

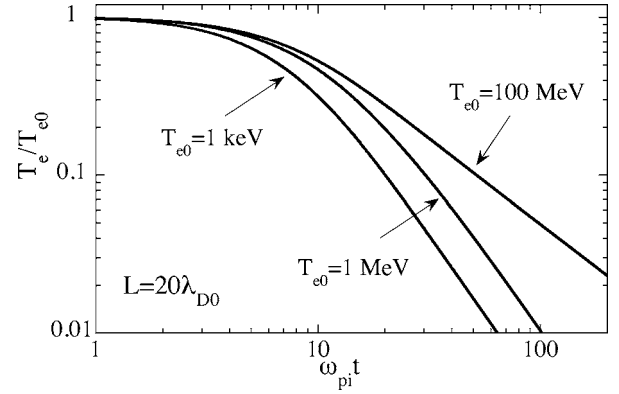


FIG. 2. Electron temperature as a function of time for $L=20\lambda_{D0}$ and $T_{e0}=1$ keV, 1 MeV, and 100 MeV.

sidered as a function of the Lagrangian position, except for the ion front for which the local Debye length is the relevant characteristic length. Note that here the self-similar character is only acquired in the limit $t \gg t_L$ in contrast to the self-similar character of the solutions of Ref. [11], which is true for any time due to the specific initial conditions and the quasineutral assumption. The asymptotic behavior of the electron temperature can be obtained from (3) with $v_e \approx x/t$, giving $dT_e/dt = -T_e/g(\theta)t$, and thus $T_e \propto t^{-2}$ for $g \approx 1/2$, as observed in Fig. 2, which shows the time dependence of the electron temperature for the parameters of Fig. 1. Also shown for comparison are, on one hand, the nonrelativistic case $T_{e0}=1$ keV, which corresponds to a faster cooling, due to a smaller initial value of θ and thus of $g(\theta)$, and, on the other hand, the ultrarelativistic case $T_{e0}=100$ MeV, which corresponds to $g \approx 1$, giving $dT_e/dt = -T_e/t$ and thus $T_e \propto t^{-1}$. Note that the nonrelativistic asymptotic $T_e \propto t^{-2}$ scaling is a general law which is verified by all the previous studies of one-dimensional (1D) adiabatic expansion into a vacuum of a collisionless plasma [11,12,14].

Figure 3 shows the time dependence of the velocity of the fastest ions for the parameters of Fig. 1. Also shown in dotted line is the prediction of Eq. (1). It is interesting to note that, at time $t=t_L$, the electron temperature is approximately 47% of its initial value, while the fastest ions have gained 50% of their final energy.

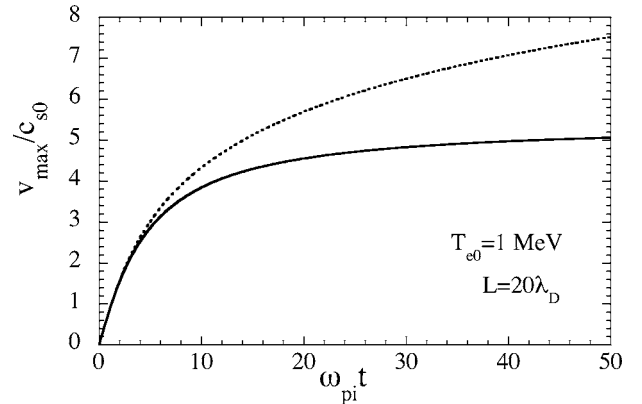


FIG. 3. Fastest ions velocity as a function of time for $L=20\lambda_{D0}$ and $T_{e0}=1$ MeV. Also shown in dotted line is the prediction of Eq. (1). The final value of v_{max} is 5.40.

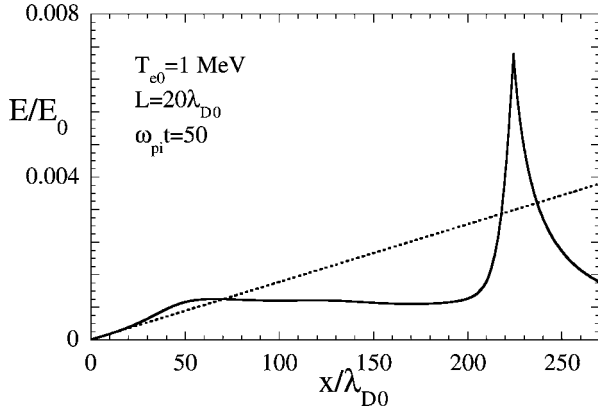


FIG. 4. Electric field as a function of x for $L=20\lambda_{D0}$ and $T_{e0}=1$ MeV, at time $\omega_{pi}t=50$. E is normalized to $E_0=(n_{e0}k_B T_{e0}/\epsilon_0)^{1/2}$. The dotted line is the electric field corresponding to the best-fitted Gaussian density of Fig. 1.

Figure 4 shows the electric field $E=k_B T_e/e l_e(x,t)$ as a function of x for the same parameters as Fig. 1. One observes three regions in the expansion. First, the electric field increases linearly as predicted by the fully self-similar solution of Ref. [11]. This linear behavior also corresponds to the Gaussian density fit plotted in dotted line in Fig. 1. Second, in a plateau region, the electric field is almost homogeneous. As $T_e \propto t^{-2}$ and $l_e(x,t) \propto t$, one has $E \propto t^{-3}$ in the plateau region. Finally, the ion front is characterized by a peak of the electric field $E_{front} = \sqrt{2} k_B T_e / e \lambda_D \propto t^{-2}$. In the ultrarelativistic regime, the scalings would be $E \propto t^{-2}$ in the plateau region and $E_{front} \propto t^{-3/2}$. Contrary to the isothermal semi-infinite plasma case, the Debye length at the ion front is not increasing indefinitely with time, but saturates to a value which is of the order of a fraction of the initial width L (when $L \gg \lambda_{D0}$).

The ratio $E_{front}/E_{plateau}$ which is equal to 2 in the isothermal semi-infinite model is now increasing linearly with time, so that the double layer staying at the ion front becomes the

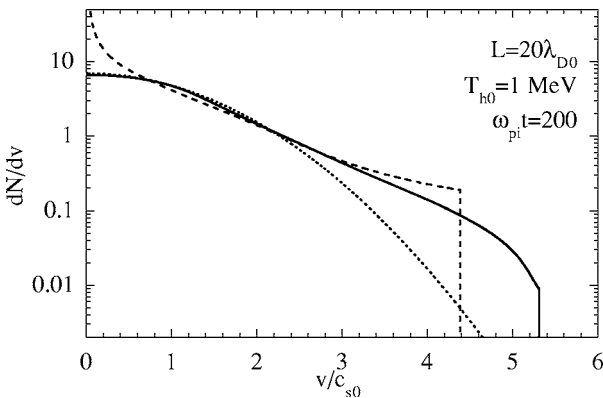


FIG. 5. Velocity spectrum per unit surface at $\omega_{pi}t=200$. Velocity is normalized to c_{s0} , and the number of ions per unit surface and unit velocity is normalized to $n_{i0}\lambda_{D0}/c_{s0}$. Also shown in dashed line is the spectrum deduced from the semi-infinite isothermal model and corresponding to the same total kinetic energy of the ions, i.e., where the velocities are frozen at time $\omega_{pi}t=10.52$. The dotted line is the Maxwellian spectrum corresponding to the fully self-similar solution of Ref. [11].

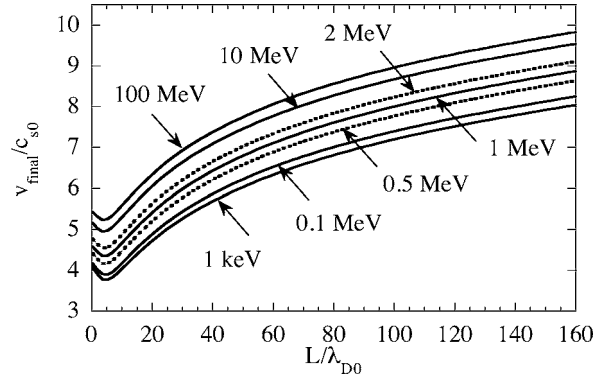


FIG. 6. Final velocity as a function of the target thickness for T_{e0} ranging from 1 keV (nonrelativistic limit) to 100 MeV (ultrarelativistic limit).

dominant feature of the electric field structure at late times. Recent experimental results of probing of high-energy protons accelerating fields in short-pulse laser solid interaction have evidenced the existence of such a double layer [15].

Figure 5 shows the ion velocity spectrum at $\omega_{pi}t=200$, which can be considered as almost final, as T_e has fallen down to $T_{e0}/400$. Also shown in dashed line is the spectrum deduced from the semi-infinite isothermal model and corresponding to the same total kinetic energy of the ions, i.e., corresponding to $\omega_{pi}t=10.52$, which is approximately $t=t_L$. Note that the fastest part of the spectrum extends to a cutoff which is approximately 20% larger in the adiabatic case than in the isothermal case. The dotted line is the Maxwellian spectrum corresponding to the fully self-similar solution.

Figure 6 shows the final velocity as a function of the target thickness for T_{e0} ranging from 1 keV (nonrelativistic limit) to 100 MeV (ultrarelativistic limit). For $L \geq 20\lambda_{D0}$, a logarithmic fit conveniently represents the results. In the nonrelativistic limit, one has

$$v_{final} \simeq 2c_{s0} \ln(0.32L/\lambda_{D0} + 4.2). \quad (4)$$

The numerical values appearing in the argument in Eq. (4) are slight functions of T_{e0} , because of relativistic effects. For

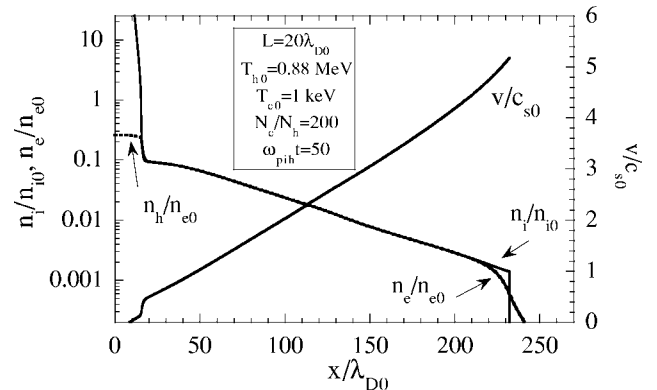


FIG. 7. Ion, total electron and hot electron densities, and ion velocity as functions of x in the two-temperature case, for $L=20\lambda_{D0}$, $T_{h0}=0.88$ MeV, $T_{e0}=1$ keV, and $N_e/N_h=200$, at time $\omega_{pi}t=50$. The total energy is identical to the case of Figs. 1–5. The normalizations are the same as in Figs. 1–5.

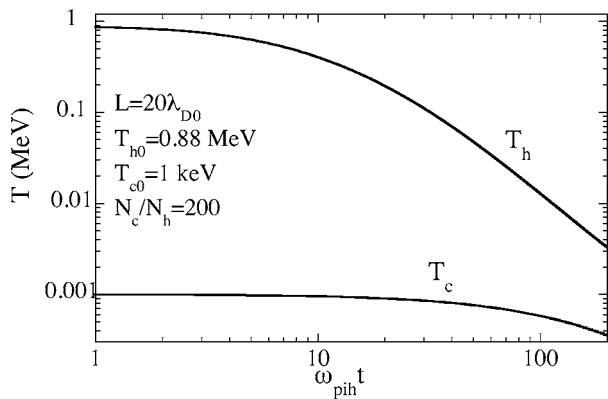


FIG. 8. Electron temperatures as functions of time in the two-temperature case.

instance, for $T_{e0}=1$ MeV, the respective values are 0.49 and 5.3 and for $T_{e0}=100$ MeV, the respective values are 0.80 and 8.17. It is important to make two remarks. First, when $L/\lambda_{D0} \gg 1$, Eq. (4) is similar to Eq. (1) with $t \approx t_L$. Second, the L dependence of v_{final} is given for constant values of the parameters T_{e0} and n_{e0} , which corresponds to a situation where the number of electrons N_e and the total initial electron energy U_e are also linearly increasing with L (ideally it corresponds to a laser pulse energy which also increases with L). In an experiment where the target width is varied for a fixed laser pulse, n_{e0} is normally a strongly decreasing function of the width [2], and the Debye length λ_{D0} increases strongly with L , so that L/λ_{D0} in fact decreases when L increases, and the curve of Fig. 6 is explored backwards. When L goes to 0, v/c_{s0} goes to a finite value. The fact that v/c_{s0} initially decreases when L increases is due to the fact that the available energy per ion is decreasing, since the ratio of the electrostatic energy to the total energy in the initial condition goes from $1/(1+g)$ when $L=0$ to 0 when L goes to ∞ .

Up to now, we have ignored the presence of cold electrons in the foil and all our discussion was based on a single population of (hot) electrons. The model has been completed by cold electrons which are assumed to satisfy a Boltzmann equation corresponding to a cold temperature T_c , while T_h now refers to the hot electrons [16]. Let N_c and N_h be the corresponding number of electrons. In the following, to facilitate the comparison with the previous one-temperature case, all the normalizations are based upon the hot electrons component, i.e., the electron densities are normalized to $n_{e0} = N_h/L$, the ion density is normalized to $n_{i0} = n_{e0}/Z$, and we define a partial ion plasma frequency $\omega_{pih} = (N_h Z e^2 / m_i \epsilon_0 L)^{1/2}$, while c_{s0} corresponds to a 1 MeV temperature and $\lambda_{D0} = c_{s0} / \omega_{pih}$. The evolution of the cold temperature is determined by Eq. (3) while the evolution of the hot temperature can be determined by Eq. (3) or alternatively by Eq. (2). The physical values of T_{h0}/T_{c0} and N_c/N_h are very large but are still tractable in our numerical model. We have chosen the values $T_{h0}/T_{c0} = 880$ and $N_c/N_h = 200$, which

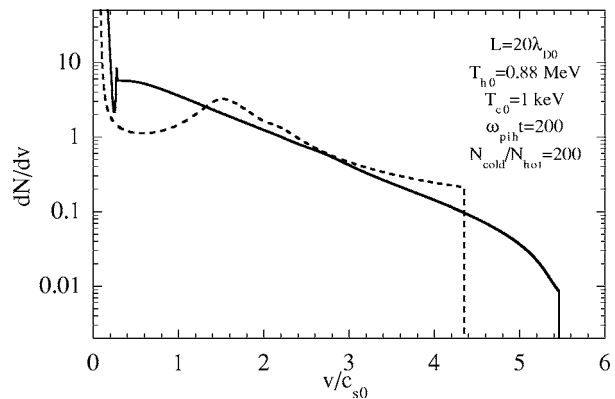


FIG. 9. Velocity spectrum per unit surface at $\omega_{pih}t=200$ in the two-temperature case. Also shown in dashed line is the spectrum deduced from the semi-infinite two-temperature isothermal model and corresponding to the same total kinetic energy of the ions, i.e., where the velocities are frozen at time $\omega_{pih}t=8.25$.

are in the regime where the electron pressure is dominated by the hot electrons and where the ratio T_h/T_c is well above the critical value $5 + \sqrt{24} \approx 9.9$ for which the quasineutral fluid theory of the expansion of a semi-infinite plasma predicts a rarefaction shock separating two regions in the expansion, dominated respectively by cold and hot electrons [17]. The choice $T_{h0}=0.88$ MeV is such that the total energy in the foil is the same as in the previous one-temperature case.

Figure 7 shows the ion and electron densities and the ion velocity as functions of x at time $\omega_{pih}t=50$. First, the expansion is clearly divided into two regions, corresponding respectively to cold-dominated and hot-dominated parts. Second, the low density, high velocity part is almost identical to what it was in the one-temperature case (see Fig. 1). Note that the rarefaction wave, which is mainly governed by the cold electrons, has not yet reached the center of the foil at that time.

Figure 8 shows the two electron temperatures as functions of time. Note that the hot temperature decays almost as in the one-temperature case (compare with Fig. 2) while the cold temperature decays slower, at least initially.

Figure 9 shows the ion velocity spectrum (full line), which is almost identical to what it was in the one-temperature case (see Fig. 5) in its high velocity part. Thus, as expected, the fast ion expansion is mainly determined by the hot electrons component. Also shown in dashed line is the two-temperature case corresponding to a semi-infinite plasma, i.e., with no time variation of T_h and T_c , and where the velocities have been frozen at time $\omega_{pih}t=8.25$, for which the total energy in the ion spectrum is the same. Note that the dip, which is present at low velocity in the semi-infinite plasma two-temperature case, is almost absent in the thin foil, time-dependent two-temperature case.

Finally, the relevance of the isothermal model and of the present adiabatic model to experiments is now briefly discussed. An essential parameter is the ratio of the pulse duration t_l to the time it takes to the hot electrons created at the front surface to completely fill the foil, i.e., $t_e = 2L/c$ (for $L = 47 \mu\text{m}$, $t_e = 320$ fs). When $t_l \ll t_e$, the hot electrons' burst interacts only once with the rear target and the isothermal

model applies with $t=t_l$. On the other hand, when $t_l \simeq t_e$, the hot electrons completely fill the target and the adiabatic model applies. When $t_l > t_e$, the adiabatic model applies as a first approximation, but can be improved by adding a source

(heating) term on the right-hand side of Eqs. (2) and (3).

The author acknowledges the fruitful comments of J. Fuchs.

-
- [1] E. L. Clark *et al.*, Phys. Rev. Lett. **84**, 670 (2000); A. Mak-simchik, S. Gu, K. Flippo, D. Umstadter, and V. Y. Bychenkov, Phys. Rev. Lett. **84**, 4108 (2000); R. A. Snavely *et al.*, Phys. Rev. Lett. **85**, 2945 (2000); J. Badziak, E. Woryna, P. Parys, K. Y. Platonov, S. Jabionski, L. Ryc, A. B. Vankov, and J. Wolowski, Phys. Rev. Lett. **87**, 215001 (2001); A. J. Mackinnon, Y. Sentoku, P. K. Patel, D. W. Price, S. Hatchett, M. H. Key, C. Andersen, R. Snavely, and B. R. Freeman, Phys. Rev. Lett. **88**, 215006 (2002); M. Hegelich *et al.*, Phys. Rev. Lett. **89**, 085002 (2002); M. Roth *et al.*, Phys. Rev. ST Accel. Beams **5**, 061301 (2002); J. Fuchs *et al.*, Phys. Rev. Lett. **94**, 045004 (2005).
- [2] M. Kaluza, J. Schreiber, M. I. K. Santala, G. D. Tsakiris, K. Eidmann, J. Meyer-ter-Vehn, and K. J. Witte, Phys. Rev. Lett. **93**, 045003 (2004).
- [3] Y. Sentoku *et al.*, Phys. Plasmas **10**, 2009 (2003).
- [4] L. O. Silva, M. Marti, J. R. Davies, R. A. Fonseca, C. Ren, F. Tsung, and W. B. Mori, Phys. Rev. Lett. **92**, 015002 (2004).
- [5] S. P. Hatchett *et al.*, Phys. Plasmas **7**, 2076 (2000).
- [6] S. C. Wilks, W. L. Kruer, M. Tabak, and A. B. Langdon, Phys. Rev. Lett. **69**, 1383 (1992).
- [7] S. C. Wilks *et al.*, Phys. Plasmas **8**, 542 (2001); A. Pukhov, Phys. Rev. Lett. **86**, 3562 (2001).
- [8] A. V. Gurevich, L. V. Pariiskaya, and L. P. Pitaevskii, Zh. Eksp. Teor. Fiz. **49**, 647 (1965) [Sov. Phys. JETP **22**, 449 (1966)]; J. E. Crow, P. L. Auer, and J. E. Allen, J. Plasma Phys. **14**, 65 (1975).
- [9] P. Mora and R. Pellat, Phys. Fluids **22**, 2300 (1979).
- [10] P. Mora, Phys. Rev. Lett. **90**, 185002 (2003).
- [11] D. S. Dorozhkina and V. E. Semenov, Phys. Rev. Lett. **81**, 2691 (1998); A. V. Baitin and K. M. Kuzanyan, J. Plasma Phys. **59**, 83 (1998); V. F. Kovalev, V. Yu. Bychenkov, and V. T. Tikhonchuk, JETP **95**, 226 (2002); V. F. Kovalev and V. Yu. Bychenkov, Phys. Rev. Lett. **90**, 185004 (2003).
- [12] M. A. True, J. R. Albritton, and E. A. Williams, Phys. Fluids **24**, 1885 (1981).
- [13] S. Betti *et al.*, Plasma Phys. Controlled Fusion **47**, 521 (2005).
- [14] G. Manfredi, S. Mola, and M. R. Feix, Phys. Fluids B **5**, 388 (1993).
- [15] L. Romagnani *et al.*, Phys. Rev. Lett. **95**, 195001 (2005).
- [16] M. Passoni, V. T. Tikhonchuk, M. Lontano, and V. Y. Bychenkov, Phys. Rev. E **69**, 026411 (2004).
- [17] B. Bezzerides, D. W. Forslund, and E. L. Lindman, Phys. Fluids **21**, 2179 (1978); L. M. Wickens, J. E. Allen, and P. T. Rumsby, Phys. Rev. Lett. **41**, 243 (1978).